Concept and laboratory testing of a pedestrian bridge span constructed from a repurposed wind turbine blade

M. Kulpa[1*], M. Rajchel[1], and T. Siwowski[1]

[1] Department of Road and Bridges, Rzeszow University of Technology , Rzeszow, Poland

* *Corresponding author (kulpa@prz.edu.pl)*

Keywords: *Bridge; Footbridge Span; Wind Turbine Blade; Reusing; Civil Engineering*

1. Abstract

The wind energy sector faces a massive disposal problem as the first generation of wind turbine blades reaches the end of its 20-25 year lifespan. Reusing these large composite components in their current state is highly preferred. This paper presents the concept of repurposing wind blades as primary load-bearing bridge girders. The research involved developing conceptual drawings, followed by a detailed geometry simulation of the finale structure. A dedicated concrete deck slab was designed to integrate with the composite blade. To maximize material utilization, ground-up composite waste from non-structural parts of the blade was embedded into the concrete mix. Additionally, the deck was reinforced with composite rebars instead of steel. A novel, original connection method between the composite and concrete parts was developed and validated through small-scale model tests. Furthermore, comprehensive material testing was conducted on samples from actual 25-year-old turbines to assess their residual mechanical quality. Based on these data, technical documentation was prepared to fabricate a full-scale, 9-meter demonstration hybrid girder prototype. The paper concludes with the experimental results and load values obtained during laboratory testing of this full-size element.

2. Introduction

The service life of FRP wind turbine blades (WTBs) is typically limited to 20 years due to harsh environmental conditions and fatigue loading. Additionally, upgrading wind farms with larger turbines leads to the decommissioning of thousands of blades. Structural recycling offers a promising end-of-life (EoL) solution by reusing decommissioned WTBs (dWTBs) as large construction components, preserving their structural integrity with minimal reprocessing effort [1, 2]. While various R&D projects reuse dWTBs for urban furniture or housing, recent research focuses heavily on civil engineering structures, such as bridges [2, 3]. Notably, the world's first bridge utilizing dWTBs was installed in late 2021 in Szprotawa, Poland, resulting from a collaboration between the recycling company Anmet and Rzeszów University of Technology (RUT) [4].

The primary objective of the ongoing RUT project is to develop, design, and implement a hybrid bridge girder combining a Vestas V-66 dWTB with concrete for pedestrian or small road bridges. This paper presents the conceptual design, terrestrial laser scanning of blade geometry, material testing, finite element modeling, and laboratory structural testing of full-scale girders. Recent results demonstrate that the proposed repurposing method is both feasible and highly promising.

3. The concept of a hybrid bridge span

The concept assumes the use of the Vestas V-66 dWTB type. The V-66 dWTBs, produced by Danish Wind System A/S, were decommissioned after more than 20 years of service in Germany. A single V-66 wind turbine blade is about 30 m long, and its edge-oriented depth ranges from 1460 to 2750 mm. The V-66 wind turbine blade is made of E-glass fibres and an epoxy resin matrix. Cross sections along the wind blade have three main subcomponents: the shell (the skin, which defines the airfoil shape), and the box girder, which consists of the spar caps and shear webs. The shell and the girder webs are made of sandwich composites, whereas the spar cap in the box girder is made of solid composites. In this case, the leading edge of the airfoil is also made of solid composites.

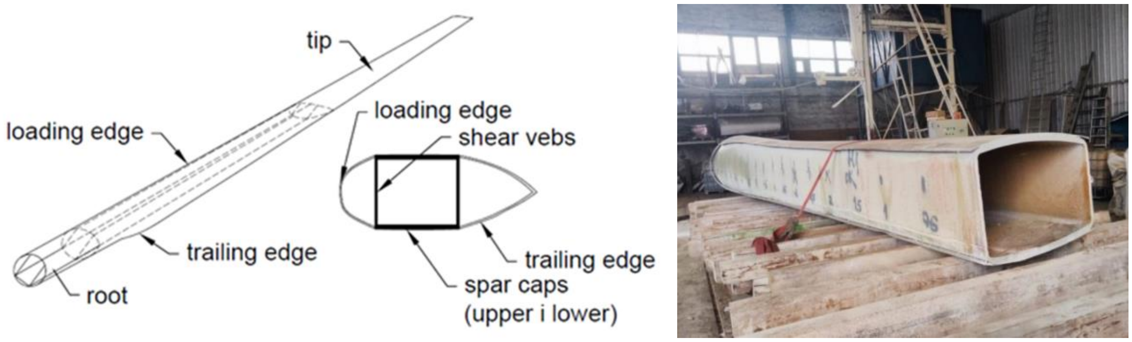

Figure 1. The V-66 hybrid bridge girder concept: a box girder section cut from a decommissioned wind turbine blade (left) and the actual element after cutting (right)

For construction of the hybrid bridge girder, the tip and root of the dWTB are first cut off to achieve the specified girder length. Then, the shell is cut off longitudinally to form a FRP box girder with two horizontal spar caps (upper and lower) and two vertical shear webs (Fig. 1, left). The FRP box acts as a key component of the hybrid bridge girder, with the spar caps serving as the main flanges that carry loads. To connect the box girder to the concrete slab, shear studs made of M-20 class 8.8 bolts are inserted into holes in the girder's upper surface and tightened with two nuts. These shear studs are installed in pairs at intervals of 0.3 m along the girder's length. In the support zones of the blade section, identical shear studs linking the girder to the concrete support blocks are also installed. Subsequently, a 0.18 m-thick slab and two support blocks measuring 0.5 × 1.5 m are cast within formwork supported by a girder. The slab and blocks are supposed to be made from an unconventional concrete of class C35/45, with 5% of the coarse aggregate by weight replaced by crushed chips from blades, with a maximum size of 3 cm. The girder's concrete elements are reinforced with 10 mm or 12 mm GFRP bars.

The concept of the simple supported V-66 bridge span, typically constructed with eight hybrid girders, has a maximum span length of 10 m, a deck width of 10.5 m, and a girder axial spacing of 1.25 m. The thickness of the slab is assumed to be 0.18 m, and the depth of the concrete end cross-beams at supports is 1.50 m.

4. The geometry and properties of the V-66 blades

The complete geometry of the 16.0 m section of V-66 dWTB was captured using a Surphaser 25HSX phase-shift terrestrial laser scanner (TLS). One-sided scans were performed at approximately 5.0 m intervals, positioning the device to maximize the visibility of overlapping regions and characteristic features. Initial alignment was performed using 4–6 common points, followed by precise registration using several thousand overlapping cloud points. The resulting point clouds were cleaned and exported as XYZ coordinates to generate a complex 3D model of the blade (Fig. 2).For material characterization, the blade section was divided into sixteen 1.0 m segments to extract samples from the primary load-carrying components: the spar caps and shear webs. To determine the FRP laminate stacking sequence, 50 × 50 mm samples were calcined in a muffle furnace at 600°C for 60 minutes. Mechanical properties were evaluated using 6 to 8 samples collected at 2.0 m sections along six longitudinal lines. The average mechanical parameters for the spar cap and shear webs, calculated as the arithmetic mean of all samples across the blade length were used to determine composite materials in numerical model of entire designed span (Fig. 2, right).

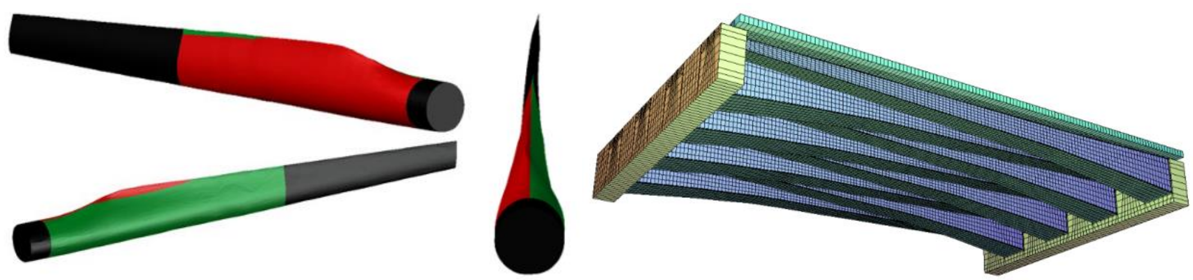

Figure 2. A result of TLS measurement: the complex 3D model of the blade (left) and FE model of a bridge with the V66 dWTB's (right)

5. The full-scale structural testing of V-66 WTB bridge girder

5.1. Full-scale model preparation

The full-scale hybrid girder measuring 9.3 m was prepared for structural testing. The FRP box girder was cut off from the actual dWTB using diamond saws. The first cut was made at a section 2.7 m from the root, while the second was at 8.8 m from the first cut. The blade shell was then cut off longitudinally to create a box girder comprising both spar caps and shear webs (Fig. 3, left). The girder's cross-section varies from round to square, with a depth of 0.5 to 1.25 m and a width of 0.66 to 1.25 m. The shear studs made of M-20 class 8.8 bolts were inserted into holes in the upper surface and in the support zones of the girder. Subsequently, a 0.18 m-thick slab and two support blocks measuring 0.5×1.7×2.21 m were cast. The girder's concrete elements were reinforced with GFRP bars. The full-scale hybrid girder model for structural testing is presented in Fig. 3.

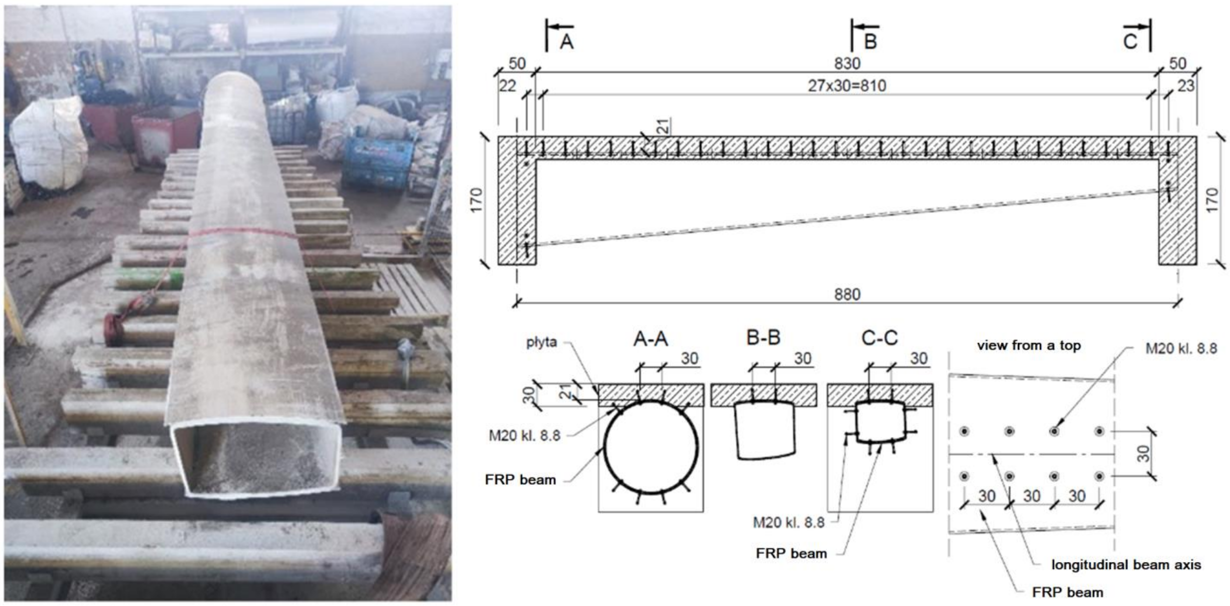

Figure 3. Composite beam obtained from a dWT (left) and the geometry of the prototype girder

5.2. Test setup and instrumentation

The static test of the hybrid girder was performed using a four-point bending setup with two hydraulic actuators, each capable of applying a maximum force of 625 kN. The distance between the actuators was 1.4 m. To ensure effective load transfer from the hydraulic actuators to the girder, two steel load distribution cross-beams were used. The full-scale testing model was supported by two steel bearings (Fig. 4, left).

During the static test, displacements and strains were measured at key points and cross sections of the girder. A total of 62 spot sensors assessed the girder's behaviour under static load (Fig. 4, right). Vertical deflection was recorded using 18 linear variable differential transformers (LVDTs) positioned at the bottom and soffit of the girder (marked P). Four dial devices controlled the movement of the support blocks (marked H). The strains were measured with 44 foil gauges, each having a measurement base of 10-30 mm (not shown). All data were collected using the HBM Spider acquisition system with the QuantumX amplifier kit. All measurements were recorded at a sampling frequency of 2 Hz.

Furthermore, distributed fibre optic sensors (DFOS) were used to continuously monitor strains in the composites and concrete along the girder's length and depth (marked F). A total of 8 DFOS sensors (single-mode telecom-grade optical fibres) were employed, with 10 mm virtual measurement sections spaced every 10 mm along the fibres. Four longitudinal horizontal fibres were glued on the FRP box girder surface and two more onto the side surface of the concrete slab. Vertical and diagonal fibre sensors were glued in both support zones. The Luna 4600 optical backscatter reflectometer (OBR), which relies on linear Rayleigh scattering, was utilised for distributed strain measurement.

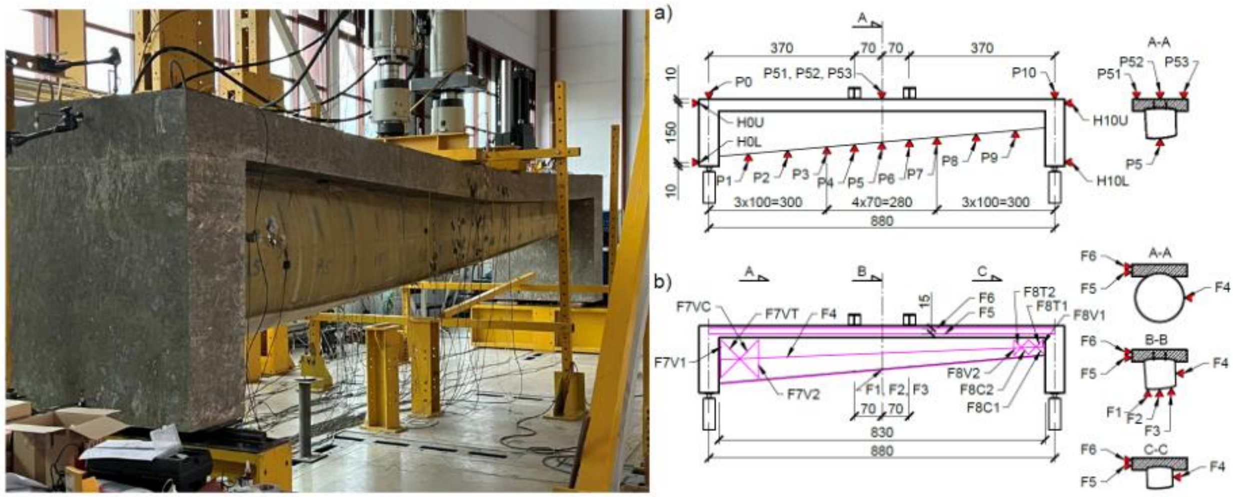

Figure 4. Prototype girder during laboratory testing (left) and the arrangement of displacement sensors (right "a") and fiber-optic sensors (right "b")

5.3. Testing program

The static girder test was carried out in six stages. The test loads for each stage were determined to match the internal forces at midspan and support, calculated in the bridge design following the previously mentioned assumptions (total length and width, service load etc.). Before starting the static test, the girder was preloaded with 2 × 50 kN to adapt it to support conditions. The load was applied at a rate of 15 kN/min. The maximum load within each cycle of a given test stage was maintained for approximately five minutes. Load control was monitored in real-time via the actuator piston and the dynamometer. After each stage, the girder was visually inspected for any signs of damage.

Table 1. Girder's testing program

Test stage	Design internal force	**Value**	**Corresponding test load**
I	Initial load	50 kN	2 × 50 kN
II	Characteristic bending moment (midspan)	443 kNm	2 × 120 kN
III	Design (factored) bending moment (midspan)	598 kNm	2 × 162 kN
IV	Characteristic transverse force (support)	298 kN	2 × 298 kN
V	Design (factored) transverse force (support)	402 kN	2 × 402 kN
VI	Maximum load at the testing stand	630 kN	2 × 630 kN

6. Test results

6.1. Deflections

The girder deformation shape is illustrated in Fig. 5 at selected loading stages. It is important to note that the LVDTs were removed before the final stage VI to protect them from destruction. However, the load applied in stage V (2 × 402 kN) was approximately 2.5 times greater than the maximum design (factored) load for the bridge; thus, the deflection results are sufficiently representative for evaluating the girder's stiffness and behaviour under static load. The shapes are derived by straightforwardly connecting displacements measured at various sections along the girder’s length. In this figure, the measured girder deformations seem consistent, and the deflected shapes are roughly symmetrical about the midsection. No significant changes in the deflected shapes under the applied loads, nor noticeable structural degradation, were observed. The maximum deflections of the girder at the load levels corresponding to the characteristic and design (factored) bending moments for the relevant load combinations (stages II and III) were 6.75 mm and 9.25 mm, respectively. However, the maximum deflection was observed not at the centre of the girder span, but at an offset of approximately 0.7 m (P-6). Notably, the first value, approximately 1/1304 of the girder length, indicates a very high girder stiffness, exceeding the bridge requirement (L/800) by a significant margin. Fig. 6 also presents a load–displacement plot for the bottom flange of the girder at P-6 point in stage V. The girder exhibited full linear-elastic behaviour until the total applied load reached 800 kN. Moreover, the residual displacement after unloading in stage V was minimal.

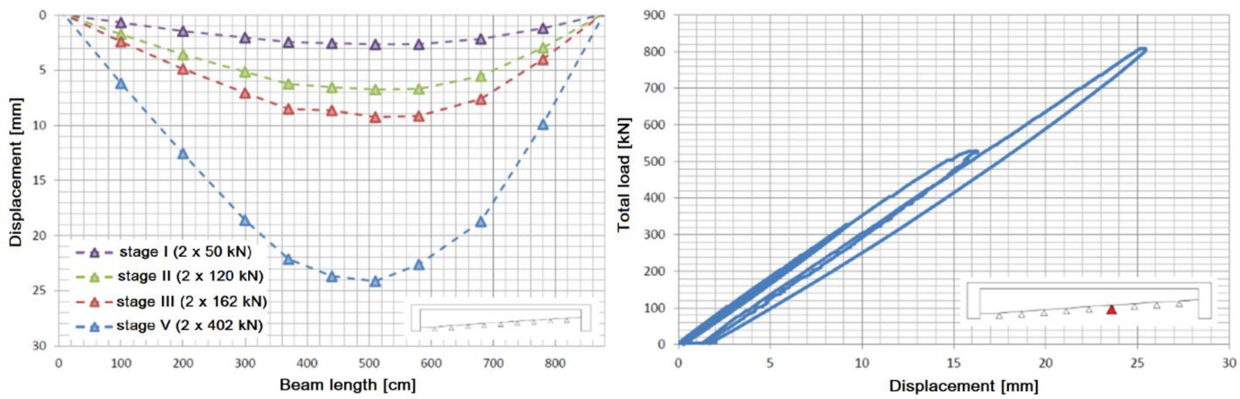

Figure 5. The girder deformation shape at selected loading stages (left) and the load–displacement plot for the bottom flange of the girder at P-6 point in stage V (right).

6.2. Strains

The strains in the main girder’s composite zones, measured by foil strain gauges, are documented elsewhere due to limitations in text length. However, exemplary results from DFOS strain measurements are shown here, illustrating the main benefits of this innovative strain measurement method. The strain distributions along the selected optical fibres are shown in Fig. 6, with strain profiles in the bottom flange of the girder (left) and the shear web (right). The strain profiles clearly demonstrate that both the overall girder response and local effects can be observed, which cannot be captured with traditional spot measurements.

Figure 6 (left) shows that the greatest variation of longitudinal strains occurs along the spar cap axis, while the strain variation at the edges is much lower due to the stiffening effect of shear webs. Additionally, significantly larger differences in strain are observed on the half of the girder with a lower depth, due to the asymmetrical cross-section in this area. Longitudinal strains in the shear web reach their highest values near the centre of the girder span (Fig. 7, right). These values are similar to those in the bottom flange (spar cap). This suggests that the web, over its larger area, was in tension. This is particularly evident in the lower depth section of the girder.

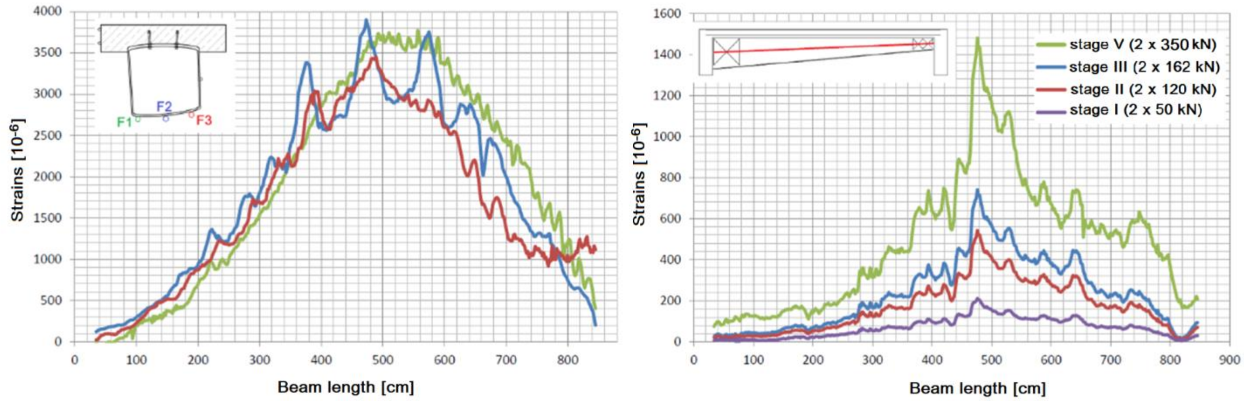

Figure 6. The girder deformation shape at selected loading stages (left) and the load–displacement plot for the bottom flange of the girder at P-6 point in stage V (right)

6.3. Failure mode

Under a maximum load of 1260 kN, the girder showed no overall failure. However, it experienced one severe local damage at 1205 kN in stage VI. During this loading stage, a loud sound was attributed to the local fracture of the shear web at the lower end of the girder (Fig. 8, left). Visual inspection after unloading revealed a 1500-mm-long one-sided fracture at the support (Fig. 7, right). The fracture occurred at a manufacturing flaw in the girder. When cutting away the shell with a diamond saw, the shear web was superficially damaged on one side over approximately 2.0 m. The linear laminate damage was about 5 mm deep, affecting both the outer skin and the core of the sandwich composite. Despite this local damage, the girder continued to carry a load of up to 1260 kN.

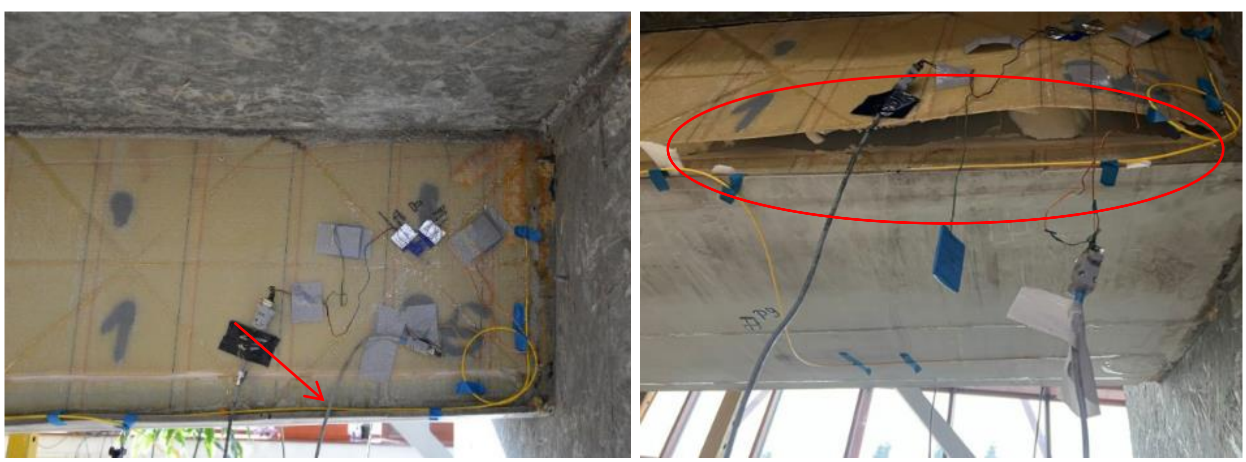

Figure 7. The support zone in the lower depth end of the girder (left) and the failure mode (local fracture) of the shear web in this support zone (right)

The strain analysis showed that the strain fields in the shear web under maximum load were well below the ultimate strength of the web sandwich composites (Fig. 7, right). The strains in the shear webs, measured with foil strain gauges, are documented elsewhere due to space limitations.

This also confirms that the local damage to the shear web had no effect on the girder's overall static behaviour. However, the girder's ultimate capacity was estimated at 1206 kN. The corresponding bending moment is therefore 2230 kNm, and the global safety factor, determined from the comparison of the ultimate moment to the characteristic design bending moment, is 5.03 (2230/443 kNm).

The remaining FRP composite girder showed no signs of deformation or delamination under maximum load, and no cracks or delamination were observed after unloading. Additionally, no visual failures were seen in the concrete slab and support blocks. This suggests that embedding the blade ends in concrete, covering the girder with the concrete slab, and mechanically fastening both with shear studs is an effective method for producing the dWTB girder for bridge applications.

7. Conclusions

This paper presents the selected results of research on dWTBs for use in bridge construction. The significant findings of the research are as follows: the experimentally determined material parameters of the composites extracted from the dWTB, which can be used directly in the design and assessment of the strength, stiffness, global safety factor, and fatigue life of bridge girders made from wind turbine blades. The research reveals that all these structural characteristics of this type of hybrid girder were very high and definitely sufficient for bridges. All characteristics are compared to the relevant values of existing FRP girders (in bridge engineering), demonstrating that wind turbine blades can also be used for this purpose without compromising the load-bearing capacity and serviceability of bridges made of them. The results of the present experimental investigation contribute to the overall body of knowledge of the civil engineering profession, which has to address the accumulation of wind turbine blade waste worldwide.

8. Acknowledgements

The research was performed within the following R&D projects:

“WTBridge: Hybrid girder made of recycled wind turbine blades and unconventional concrete for the construction and modernization of bridge structures, equipped with fiber-optic sensors for structure monitoring,” funded by the National Centre for Research and Development (Poland) within the framework of the LIDER Program (LIDER13/0031/2022).

“PROM – krótkookresowa wymiana akademicka”, project no. BPI/PRO/2025/1/00016, decision no. BPI/PRO/2025/1/00016/DEC/01. The project is coordinated by the Rzeszow University of Technology named Ignacy Łukasiewicz, Poland, as the Polish coordinating institution contracted with NAWA.

“Regional Excellence Initiative” program under contract no. RID/SP/0032/2024/01 entitled “Regional Center of Excellence in Engineering for Quality of Life and Technology Development”.

9. References

[1] E.L. Delaney, P.G. Leahy, J.M. McKinley, T.R. Gentry, A.J. Nagle, J. Elberling and L.C. Bank. "Sustainability Implications of Current Approaches to End-of-Life of Wind Turbine Blades—A Review". Sustainability, Vol. 15, No. 16, pp 12557, 2023.

[2] K. Ruane, V. Jaksic, L.C. Bank, T.R. Gentry, K. McDonald, M. Soutsos, F. Al-Mansour and V. Prakashi. "Testing and analysis of pedestrian bridge made of discarded wind turbine blades". Proceedings of Engineering Materials, Structures, Systems and Methods for a More Sustainable Future, pp 1537-1542, 2025.

[3] K. Ruane, V. Jaksic, L.C. Bank, T.R. Gentry, K. McDonald, M. Soutsos, C. Graham, E. Delaney, J. McKinley, P. Leahy, A. Nagle, E. Esmaeeli and V. Prakashi. "Testing and analysis of pedestrian bridge made of discarded wind turbine blades". Proceedings of Engineering Materials, Structures, Systems and Methods for a More Sustainable Future, pp 1537-1542, 2025.

[4] Rajchel, M., Kulpa M., Wiater, A., & Siwowski T. Repurposing a Decommissioned Wind Turbine Blade for Bridge Construction: An Experimental Investigation. Journal of Composites for Construction ASCE, 29(1), 2025.